



**QUEEN'S
UNIVERSITY
BELFAST**

Time-modulated OFDM Directional Modulation Transmitters

Ding, Y., Fusco, V., Zhang, J., & Wang, W-Q. (2019). Time-modulated OFDM Directional Modulation Transmitters. IEEE Transactions on Vehicular Technology, 1-3. <https://doi.org/10.1109/TVT.2019.2924543>

Published in:

IEEE Transactions on Vehicular Technology

Document Version:

Peer reviewed version

Queen's University Belfast - Research Portal:

[Link to publication record in Queen's University Belfast Research Portal](#)

Publisher rights

Copyright 2019 IEEE. This work is made available online in accordance with the publisher's policies. Please refer to any applicable terms of use of the publisher.

General rights

Copyright for the publications made accessible via the Queen's University Belfast Research Portal is retained by the author(s) and / or other copyright owners and it is a condition of accessing these publications that users recognise and abide by the legal requirements associated with these rights.

Take down policy

The Research Portal is Queen's institutional repository that provides access to Queen's research output. Every effort has been made to ensure that content in the Research Portal does not infringe any person's rights, or applicable UK laws. If you discover content in the Research Portal that you believe breaches copyright or violates any law, please contact openaccess@qub.ac.uk.

Time-modulated OFDM Directional Modulation Transmitters

Yuan Ding, Vincent Fusco, Junqing, Zhang, and Wen-Qin Wang

Abstract—In this paper directional modulation (DM) transmitters, designed for orthogonal frequency-division multiplexing (OFDM) wireless data transfer are proposed using time-modulated arrays (TMAs). It is shown that by properly designing the switch controlling time sequences the proposed time-modulated OFDM DM systems exhibit promising features, such as *i)* requires only one radio frequency (RF) chain, *ii)* the conventional efficient OFDM signal construction approach, i.e., by using inverse fast Fourier transform (IFFT) modules, can be adopted, *iii)* it is ‘DM synthesis-free’, meaning that there is no need to re-synthesize the array excitation vectors for different secure communication directions, different modulation schemes, and different DM power efficiencies; and *iv)* the trade-off between secrecy performance and power efficiency can be flexibly adjusted.

Index Terms—Directional Modulation (DM), orthogonal frequency-division multiplexing (OFDM), physical-layer wireless security, time-modulated array (TMA)

I. INTRODUCTION

Directional Modulation (DM), as a promising physical-layer secure wireless communication technique, has been rapidly developed in recent years [1]–[5]. It has the key property of transmitting digitally modulated signals whose waveforms are well preserved only along a pre-selected direction along which legitimate users locate in free space. Its evolution began with a type of architectures consisting of re-configurable, operating at the transmitted symbol rates, radio frequency (RF) components, [1], [2], [6], which have the ability of changing far-field radiation patterns, resulting in signal waveform distortions in unwanted directions. Later, digital baseband DM solutions were proposed, [3], [4], [7], which facilitate the synthesis of the DM transmitter array excitation vectors. More recent efforts were directed at practical field applications. This resulted in ‘synthesis-free’ DM architectures, such as Fourier beamforming network enabled DM [8], antenna subset modulation arrays [9], [10], retrodirective DM arrays [5], and mode-pattern circular DM arrays [11]. Here the term ‘synthesis-free’ refers to the fact that no calculation of the DM array excitation vectors is required, as the DM functionality is directly enabled through carefully constructed DM transmitter hardware.

It needs to be pointed out that most of the previous DM works only consider single carrier signals. Since multi-carrier modulation schemes, like orthogonal frequency-division multiplexing (OFDM), have been widely adopted in the modern wireless communication systems, such as IEEE 802.11 and LTE, it is worth investigating the

multi-carrier DM systems, incidentally mentioned as the future work in the review paper [12].

One approach to extending the single-carrier DM to multi-carrier DM is to synthesize multiple single-carrier DM transmitters and vectorially combine the resultant array excitations that can then be used for multi-carrier DM. In this category, a special arrangement of applying the frequency diverse array (FDA) concept onto the DM was first introduced in [13]. However, this strategy is associated with a number of issues, namely: *i)* it requires multiple RF chains, the number of which equals the number of array antenna elements. This multi-RF-chain structure is not preferred as it significantly increases the system complexity and cost, especially when higher operation frequencies are used; *ii)* as the synthesized DM excitation signals at each antenna port are not OFDM signals, they cannot be efficiently constructed using IFFT modules; and *iii)* the synthesis process needs to be re-run when the number of signal carriers, the modulation types, and the desired secure communication directions change, i.e., the approach is not ‘synthesis-free’.

Different to the afore-mentioned approach, in this paper, we exploit the unique property of time-modulated arrays (TMAs) to construct OFDM DM transmitters, which overcome the problems associated with the method presented earlier.

TMA is a technique wherein by introducing a fourth dimension, time, as an additional degree of freedom for the array design, i.e., connecting and disconnecting the antenna elements from the feeding network in time domain, the radiation pattern can be further manipulated [14]. The approach has been primarily exploited for array radiation pattern synthesis with suppressed sidelobes by shifting the signal energy projected along sidelobe directions out of the system operating frequency bands [15], [16]. Until recently, this ability of shifting the frequency of radiated signals has been found useful for a number of applications, such as direction finding [17] and space division multiple access [18]. In this paper we use this spatial frequency expansion characteristic of the TMA to secure broadcasted OFDM signals by enabling DM functionality, i.e., constructing OFDM DM transmitters. To achieve the DM functionality, namely preserving OFDM signal waveforms along selected spatial directions while distorting them in all other directions, which is equivalent to enabling the orthogonality between the information signals and the artificial interference, not only in spatial domain but also in frequency domain, the switching waveforms controlling the connection and disconnection of the array elements have to be carefully designed.

The contributions of the research presented in this paper are summarized as follows;

- The architecture of an OFDM DM transmitter, constructed using TMAs, is presented. It features single RF-chain, IFFT compatible, DM ‘synthesis-free’, and adaptable performance, which have never been studied in previous reported works;
- The required time-domain switch functions are analytically derived and validated through simulations;
- The tradeoff between array energy efficiency and secrecy performance is revealed and quantitatively investigated.

Readers who are following DM developments may be aware of a number of recent DM works, which claim that the FDA concept (and its variants such as non-linear frequency increments and random subcarrier selections) can be incorporated into DM transmitters, achieving free-space wireless security in range-domain, e.g. the random-subcarrier-selection-based OFDM DM transmitters in [19] and some of the references wherein. However, in those works one important factor was overlooked, which is that ‘FDA range-angle dependent beamforming patterns are also functions of time’. This

Copyright (c) 2015 IEEE. Personal use of this material is permitted. However, permission to use this material for any other purposes must be obtained from the IEEE by sending a request to pubs-permissions@ieee.org.

Manuscript received Sep. 20, 2018, revised Mar. 29, 2019 and Jun. 12, 2019, and accepted Jun. 20, 2019. Y. Ding’s work was supported by the Carnegie Research Incentive Grant RIG008216. V. Fusco’s work was supported by the EPSRC (UK) under Grants EP/N020391/1 and EP/P000673/1.

Y. Ding is with the Institute of Sensors, Signals and Systems (ISSS), Heriot-Watt University, Edinburgh, United Kingdom, EH14 4AS (e-mail: yuan.ding@hw.ac.uk).

V. Fusco is with the Institute of Electronics, Communications and Information Technology (ECIT), Queen’s University Belfast, Belfast, United Kingdom, BT3 9DT.

J. Zhang is with Department of Electrical Engineering & Electronics, University of Liverpool, Brownlow Hill, Liverpool, L69 3GJ, United Kingdom.

W.-Q. Wang is with University of Electronic Science and Technology of China, Chengdu 611731, China.

means that the secure reception regions (normally defined as the locations where the reception bit error rates (BERs) are below a specified threshold), erroneously claimed in those works as being fixed in angle and range domains, propagate in range as time elapses. For example take the scheme in [19] as an example, here the authors formulated the received signals acquired by the legitimate and eavesdropper receivers in (11) and (12), respectively, in [19]. It can be observed that the authors assumed that two receivers sample the signals at the same time instant, i.e., using the same viable ‘ t ’ for both receivers. This leads, as shown through simulation results, to the pencil peak of signal to interference and noise ratio (SINR) in 2-D angle-range domain. However as the authors here pointed out that the FDA radiation patterns are also time variant, meaning that the legitimate and eavesdropper receivers do not necessarily sample signals at the same time instant. In fact, in (12) when $\theta_E = \theta_D$, i.e., along the same spatial direction, if the eavesdropper receiver delays (or advances) signal samplings by $(R_E - R_D)/c$ when $R_E > R_D$, (or $(R_D - R_E)/c$, when $R_E < R_D$), (12) becomes (11). Here ‘ c ’ refers to the speed of light. This clearly indicates that the secure reception region propagates in range as time elapses. This suggests that it is impossible for any FDA enhanced DM systems to achieve free space wireless security in range domain.

It is noted in this paper that for any free space DM transmissions, the knowledge of directions of legitimate receivers needs to be acquired by the DM transmitter in advance before initiating secure transmissions. This information can be obtained by using direction of arrival (DOA) algorithms [20], or by using analogue retrodirective technologies as in [5]. This aspect is beyond the scope of this paper, thus, it will not be discussed further.

This paper is organized as follows, in Section II the architecture of the proposed time-modulated OFDM DM transmitter is presented, and the design principle is investigated. Simulation results, validating the trade-offs between the energy efficiency and secrecy performance, are provided in Section III. Finally, conclusions are drawn in Section IV.

II. PROPOSED TIME-MODULATED OFDM DM TRANSMITTER

The architecture of the proposed time-modulated OFDM DM transmitter is illustrated in Fig. 1. Apart from the input signal being OFDM modulated, it is a standard TMA system consisting of an N -element linear antenna array. It is assumed that all the antenna elements have identical isotropic active element patterns, and they are uniformly half-wavelength ($\lambda_0/2$) spaced. Here wavelength λ_0 is associated with the frequency of the first OFDM sub-carrier f_0 . The OFDM signals can be constructed using conventional IFFT modules

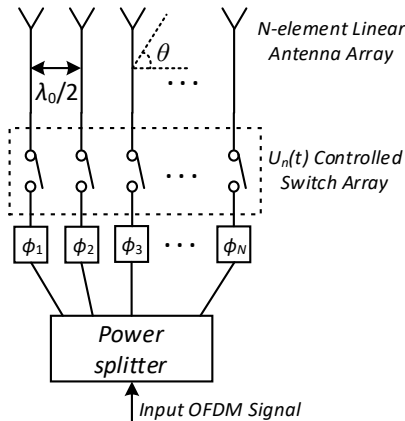


Fig. 1. Architecture of the proposed time-modulated OFDM DM transmitter.

in digital baseband, and up-converted using a single RF chain. The signals are then split into N copies with identical power. It is explained here that all OFDM subcarriers are power divided together, meaning that the power of each subcarriers in each antenna branch n is always identical, i.e. no power allocation among subcarriers. The power dividing ratio for each antenna branch, however, can be non-uniform, e.g. tapered array excitation magnitude for radiation sidelobe controls. Before being fed into their respective antenna elements, each OFDM signal copy is phase delayed and then ‘on-off’ manipulated in time domain by an RF single-pole-single-throw switch. Phase shifters steer the desired free space communication direction as in the classical phased beam-steering arrays. In order to enable the DM functionality for the OFDM signal transmission, the ‘on-off’ switching functions for each antenna branch need to be carefully selected. The method for doing this is now mathematically elaborated.

An OFDM signal can be written as

$$S(l, t) = \frac{1}{\sqrt{K}} \sum_{k=1}^K D_{kl} \cdot e^{j2\pi[f_0 + (k-1)f_p]t}, \quad (1)$$

where K is the total number of the OFDM sub-carriers, and the frequency spacing between consecutive sub-carriers is denoted as f_p . D_{kl} , normalized to be unit power, refers to the l^{th} complex modulated symbol applied upon the k^{th} sub-carrier. Unless otherwise specified, subscript ‘ l ’ is dropped hereafter in this paper, as in most cases we only consider one transmission OFDM symbol period, and the following analysis is independent to the symbol transmitted. Thus, D_k is a constant with respect to time, though being randomly selected from the adopted digital modulation constellation sets. Due to the same reason, $S(l, t)$ is referred to as $S(t)$ hereafter. The coefficient $1/\sqrt{K}$ is added in (1) for power normalization.

After being processed with the phased TMA shown in Fig. 1, the OFMA signal radiated into the half-space, $\theta \in [0, \pi]$, can be expressed as¹

$$R(\theta, t) = \sum_{n=1}^N \left(\frac{1}{\sqrt{N}} S(t) \cdot e^{j\phi_n} \cdot U_n(t) \cdot e^{j(n-1)\pi \cos \theta} \right). \quad (2)$$

Here ϕ_n is the phase delay in the n^{th} antenna branch, seen in Fig. 1. When the desired secure communication direction in free space is θ_0 , the value ϕ_n is set to be that in (3), the same as that in classical phased beam-steering arrays.

$$\phi_n = -(n-1)\pi \cos \theta_0 \quad (3)$$

It is noted here that when a multipath channel is considered, the term $e^{j(n-1)\pi \cos \theta}$ in (2) should be replaced with the channel coefficient between the n^{th} transmit element and any observation point in the radiation field. While the ϕ_n in (3) is set to the value that cancels out the phase of the channel between the n^{th} element and the legitimate receiver. The following analyses are thus applicable to multipath propagation scenarios.

$U_n(t)$ in (2) is a square waveform, controlling the ‘on-off’ of the n^{th} RF switch in time-domain, see the illustrations in Fig. 2. $U_n(t)$ of 1 (or 0) represents on/close (or off/open) of the RF switch. T_p denotes the repetition time period of the waveform, and it is set to be $1/f_p$, identical for all switches in the N branches. For the n^{th} switch, t_n^s and t_n^e refer to the ‘turn-on’ and ‘turn-off’ time instants, respectively. The ‘on’ time period is denoted as Δt_n . For the examples in Fig. 2, $\Delta t_n = t_n^e - t_n^s$

when $t_n^e > t_n^s$, or $\Delta t_n = T_p + t_n^e - t_n^s$ when $t_n^e < t_n^s$.

$U_n(t)$ can be expanded in the form of Fourier series, as

$$U_n(t) = \sum_{m=-\infty}^{\infty} c_{mn} e^{j \frac{2m\pi t}{T_p}} = \sum_{m=-\infty}^{\infty} c_{mn} e^{j 2m\pi f_p t}, \quad (4)$$

where

$$\begin{aligned} c_{mn} &= \frac{1}{T_p} \int_0^{T_p} U_n(t) e^{-j 2m\pi f_p t} dt \\ &= \begin{cases} f_p \cdot \int_{t_n^s}^{t_n^e} e^{-j 2m\pi f_p t} dt & \text{when } t_n^e > t_n^s \\ f_p \cdot \left(\int_0^{t_n^e} e^{-j 2m\pi f_p t} dt + \int_{t_n^s}^{T_p} e^{-j 2m\pi f_p t} dt \right) & \text{when } t_n^e < t_n^s \end{cases} \\ &= \frac{\sin(m\pi f_p \Delta t_n)}{m\pi} \cdot e^{-j m\pi f_p (2t_n^s + \Delta t_n)}. \end{aligned} \quad (5)$$

Substituting (1), (3), (4), and (5) into (2), we get

$$\begin{aligned} R(\theta, t) &= \sum_{n=1}^N \left[\frac{1}{\sqrt{NK}} \cdot \sum_{k=1}^K D_k \cdot e^{j 2\pi [f_0 + (k-1)f_p] t} \right. \\ &\quad \cdot \left. \sum_{m=-\infty}^{\infty} \left(\frac{\sin(m\pi \Delta \tau_n)}{m\pi} \cdot e^{-j m\pi (2\tau_n^s + \Delta \tau_n)} e^{j 2m\pi f_p t} \right) \cdot e^{j(n-1)\pi(\cos\theta - \cos\theta_0)} \right] \\ &= \left(\frac{1}{\sqrt{NK}} \cdot \sum_{k=1}^K D_k \cdot e^{j 2\pi [f_0 + (k-1)f_p] t} \right) \\ &\quad \cdot \sum_{m=-\infty}^{\infty} \left[\underbrace{e^{j 2m\pi f_p t} \sum_{n=1}^N \left(\frac{\sin(m\pi \Delta \tau_n)}{m\pi} \cdot e^{-j m\pi (2\tau_n^s + \Delta \tau_n)} \right)}_{V(m, N, \tau_n^s, \Delta \tau_n, t, \theta)} \right] \cdot e^{j(n-1)\pi(\cos\theta - \cos\theta_0)} \end{aligned} \quad (6)$$

where $\tau_n^s = t_n^s / T_p$ and $\Delta \tau_n = \Delta t_n / T_p$ are normalized switch ‘on’ time instant and the ‘on’ time period, respectively.

$R(\theta, t)$ in (6) can be regarded as the received signal along the spatial direction θ , normalized for path loss. The DM functionalities which we want to enable with the proposed TMA structure in Fig. 1 include;

- Preservation of the original transmitted signal waveform along the desire spatial direction θ_0 , which for the studied system in this paper is the OFDM waveform expressed in (1).

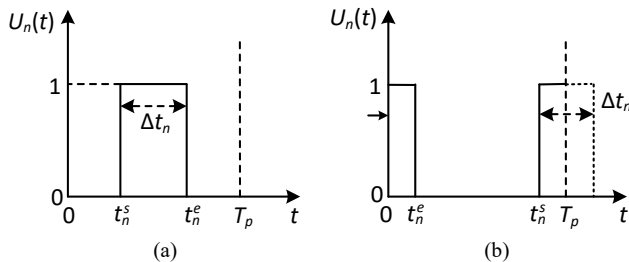


Fig. 2. Illustrations of the switch controlling waveform $U_n(t)$.

In order for this to happen, comparing (1) and (6), the following conditions have to be met,

$$V(m \neq 0, N, \tau_n^s, \Delta \tau_n, t, \theta = \theta_0) = 0 \quad (7)$$

$$V(m = 0, N, \tau_n^s, \Delta \tau_n, t, \theta = \theta_0) \neq 0 \quad (8)$$

Let us consider (7) first, which can be written as

$$\sum_{n=1}^N \left(\Delta \tau_n \cdot \text{sinc}(m\pi \Delta \tau_n) \cdot e^{-j m\pi (2\tau_n^s + \Delta \tau_n)} \right) = 0 \quad (m \in \mathbb{Z}, m \neq 0). \quad (9)$$

There exist infinite solutions to (9). As $\Delta \tau_n$ determines how much energy is preserved in the fundamental frequency component radiated by the n^{th} element in the TMA, seen in (5) when m is set to 0, we choose to make $\Delta \tau_n$ identical for each n , so that the energy efficiency of the entire TMA can be uniquely tuned by setting different $\Delta \tau$. This facilitates the illustrations of the tradeoff between array energy efficiency and secrecy performance, which will be studied in Section III. This choice results in the solution sets shown in (10).

$$\begin{cases} \tau_n^s, \Delta \tau_n \in \left\{ \frac{w-1}{N} \mid w = 1, 2, \dots, N \right\} \\ \tau_p^s \neq \tau_q^s, \Delta \tau_p = \Delta \tau_q \text{ when } p \neq q \end{cases} \quad (10)$$

The condition in (8) can be simplified as

$$\sum_{n=1}^N \Delta \tau_n \neq 0. \quad (11)$$

Since $\Delta \tau_n \in (0, 1]$, (11), and hence (8), are always satisfied.

When setting $\Delta \tau_n$ and τ_n^s according to (10), and denoting the identical $\Delta \tau_n$, with respect to different n , as $\Delta \tau$, the received OFDM signal along θ_0 becomes

$$R(\theta_0, t) = \Delta \tau \cdot \sqrt{\frac{N}{K}} \cdot \sum_{k=1}^K D_k \cdot e^{j 2\pi [f_0 + (k-1)f_p] t} = \Delta \tau \sqrt{N} \cdot S(t). \quad (12)$$

From (12) it can be observed that the normalized switch ‘on’ time period $\Delta \tau$ determines the proportion of the transmit beamforming gain, i.e., \sqrt{N} , that can be preserved. For extreme cases, when $\Delta \tau \rightarrow 0$, no gain is available as the transmitter is essentially shut down; and when $\Delta \tau \rightarrow 1$, a power gain of $10\log_{10}(N)$, in dB, is enabled as the TMA operates identically as a classical phased beam-steering array.

- Distortion of the transmitted signal waveform along the spatial directions other than θ_0 .

When $\theta \neq \theta_0$, the received x^{th} ($x = 1, 2, \dots, K$) sub-carrier is

$$\begin{aligned} R_x(\theta, t) &= \sum_{k=1}^K \left[\frac{1}{\sqrt{NK}} \cdot D_k \cdot e^{j 2\pi [f_0 + (k-1)f_p] t} \cdot V(m = x - k, N, \tau_n^s, \Delta \tau_n, t, \theta) \right], \end{aligned} \quad (13)$$

which, obviously, is corrupted by the random data that are modulated onto all the sub-carriers, and the randomly selected $\Delta\tau_n$ and τ_n^s , when (10) is satisfied.

To sum up, the constraints in (10) are the sufficient conditions to construct a time-modulated OFDM DM transmitter.

III. SIMULATION RESULTS

In order to facilitate the understanding of the operation principle of the proposed time-modulated OFDM DM transmitters, examples showing $1/\sqrt{N} \cdot |V(m, N, \tau_n^s, \Delta\tau, t, \theta)|$ in dB, denoted as Γ_m , are plotted in Fig. 3 for various parameters that satisfy (10). Operator ‘ $|\cdot|$ ’ returns the absolute value of the enclosed complex number. It can be seen from (1) and (6) that this term is the magnitude weighting coefficient along spatial direction θ applied upon the k^{th} sub-carrier of the transmitted OFDM signal, while transforming this k^{th} sub-carrier to the $(m+k)^{\text{th}}$ sub-carrier at the receiver end. In the examples in Fig. 3, we assume that the desired communication direction θ_0 equals 60° , and the linear transmit array has 7 elements, i.e., $N = 7$. It can be seen that along θ_0 the OFDM signals, including all K sub-carriers, are only radiated through Γ_0 , satisfying (7) and (8). This means the OFDM waveforms are well preserved, subject only to magnitude scaling. As predicted by (12), $\Delta\tau\sqrt{N}$ determines the achievable gain, resulting in $(2/7) \times \sqrt{7} < 1$ (lower than 0 dB) and $(4/7) \times \sqrt{7} > 1$ (higher than 0 dB), see Fig. 3. Whereas along any other directions, the received 3^{rd} sub-carrier ($x = 3$), for example, is the vectorial summation of 5 terms with magnitudes of $(1/\sqrt{5})D_1\Gamma_2$, $(1/\sqrt{5})D_2\Gamma_1$, $(1/\sqrt{5})D_3\Gamma_0$, $(1/\sqrt{5})D_4\Gamma_{-1}$, and $(1/\sqrt{5})D_5\Gamma_{-2}$. In fact, Γ_m exists for any integer m . Thus, in general case, the received x^{th} sub-carrier along directions other than θ_0 is the summation of K terms with each magnitude of $(1/\sqrt{K})D_k\Gamma_m$, subject to $k + m = x$. In addition, even for the same m and $\Delta\tau$, different choices of τ_n^s result in different Γ_m , enabling the construction of dynamic DM [21], i.e., dynamically updating orthogonal interference at symbol rates, see the examples of case1 and case2 (shown in legend) in Fig. 3.

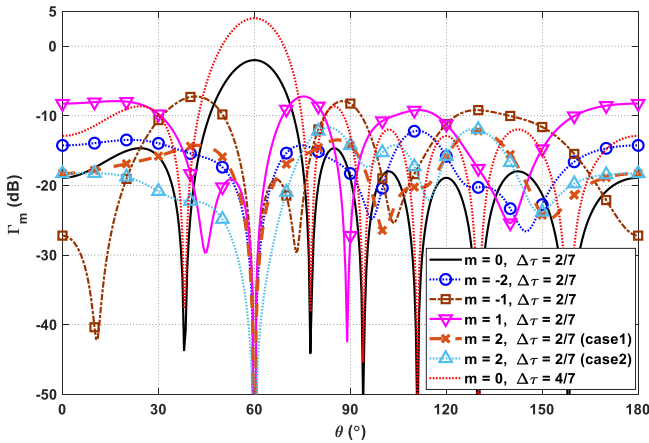


Fig. 3. Illustrations of the example Γ_m for various parameters that satisfy (10).

In Fig. 4 and Fig. 5, BER simulations across the half space, i.e., $\theta \in [0, \pi]$, are simulated for two different energy per bit to noise power spectral density ratios (E_b/N_0) for the proposed time-modulated OFDM DM systems. Here E_b/N_0 is measured along the desired secure communication direction θ_0 of 60° , and the noise power is assumed

identical along every direction. Two choices of E_b/N_0 are equivalent to different distances between transmitter and receivers that include the legitimate one along θ_0 and potential eavesdroppers along all other directions. In the examples, it is assumed that $N = 7$, $K = 64$, and the OFDM sub-carriers are QPSK modulated. It should be pointed out that the proposed time-modulated OFDM DM system works for any modulation types, as, seen in (6), the generated orthogonal (in both spatial and frequency domains) artificial noise function V is independent to the input data D_k . Due to page limits, only the QPSK modulation case is simulated and presented. The same conclusions can be reached for any other types of modulations. The case of ‘ $\Delta\tau = 1$ ’, as we discussed in the last section, refers to the corresponding conventional beam-steering array. The power efficiency of DM systems PE_{DM} , [3], [21], defined as the percentage of total radiated energy that is used to transfer useful information, can be calculated as $PE_{DM} = \Delta\tau^2 \times 100\%$. In Fig. 4, it can be observed that the signals are not corrupted along 60° , i.e., the BERs achieved at this direction are nearly identical, around 2×10^{-4} , in both DM systems and the conventional beam-steering system. Since the BER main beam is already narrow and its sidelobes are already high for the low $E_b/N_0 = 8$ dB case in Fig. 4, we increase the E_b/N_0 to 23 dB in Fig. 5, meaning the potential eavesdroppers are located much closer to the transmitter. This is done in order to demonstrate the secrecy enhancement that the DM functionality can bring. It can be clearly observed that the proposed time-modulated OFDM DM systems can help narrow the BER main beam and suppress BER sidelobes, reducing the possibility of information interception. This enhanced secrecy performance is achieved at the cost of low power efficiency, because some energy is consumed in the process of radiating orthogonal interference, both in the spatial domain and in the frequency domain.

IV. CONCLUSION

An OFDM DM transmitter was developed by exploiting the spectral expansion property of the TMA. By properly designing the time switching waveforms orthogonality between the OFDM signals to be transmitted and the dynamic artificial interference, in both spatial domain and frequency domain, can be achieved. The conditions necessary for constructing the proposed time-modulated OFDM DM transmitters have been derived, and validated through radiation patterns and BER simulations. Furthermore, the trade-off between the enhanced system secrecy performance and power efficiency has been revealed.

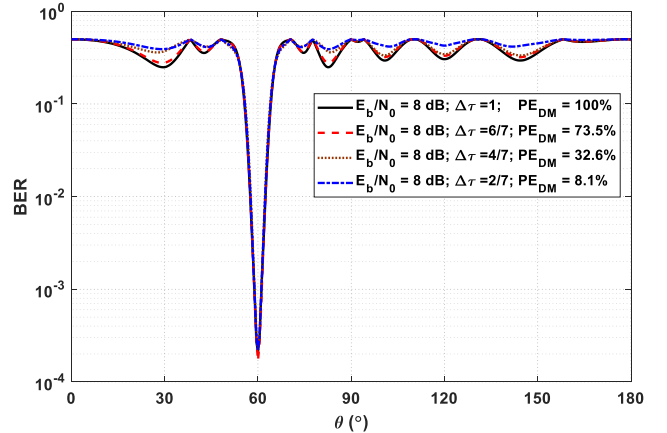


Fig. 4. Simulated BERs of the time-modulated OFDM arrays for various $\Delta\tau$ when E_b/N_0 along θ_0 of 60° equals 8 dB. ‘ $\Delta\tau = 1$ ’ refers to the conventional beam-steering array. It is assumed that each sub-carrier is QPSK modulated and $N = 7$, $K = 64$.

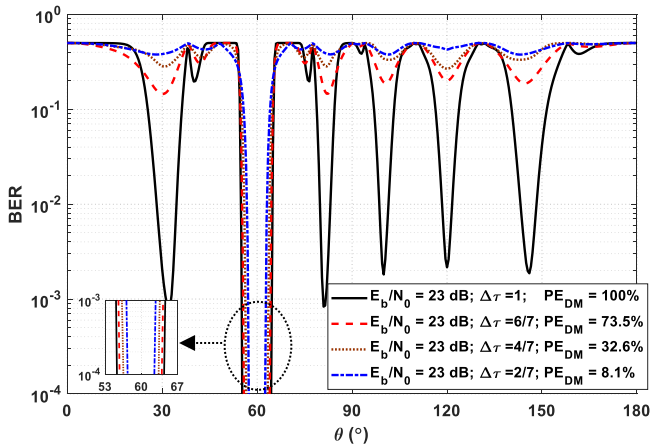


Fig. 5. Simulated BERs of the time-modulated OFDM arrays for various $\Delta\tau$ when E_b/N_0 along θ_0 of 60° equals 23 dB. ' $\Delta\tau=1$ ' refers to the conventional beam-steering array. It is assumed that each sub-carrier is QPSK modulated and $N=7$, $K=64$.

REFERENCES

- [1] A. Babakhani, D. Rutledge, and A. Hajimiri, "Near-field direct antenna modulation," *IEEE Microw. Mag.*, vol. 10, no. 1, pp. 36–46, Feb. 2009.
- [2] M. P. Daly and J. T. Bernhard, "Directional modulation technique for phased arrays," *IEEE Trans. Antennas Propag.*, vol. 57, no. 9, pp. 2633–2640, Sep. 2009.
- [3] Y. Ding and V. Fusco, "A vector approach for the analysis and synthesis of directional modulation transmitters," *IEEE Trans. Antennas Propag.*, vol. 62, no. 1, pp. 361–370, Jan. 2014.
- [4] A. Kalantari, M. Soltanalian, S. Maleki, S. Chatzinotas, and B. Ottersten, "Directional modulation via symbol-level precoding: A way to enhance security," *IEEE J. Sel. Topics Signal Process.*, vol. 10, no. 8, pp. 1478–1493, Dec. 2016.
- [5] Y. Ding and V. Fusco, "A synthesis-free directional modulation transmitter using retrodirective array," *IEEE J. Sel. Topics Signal Process.*, vol. 11, no. 2, pp. 428–441, Mar. 2017.
- [6] M. P. Daly and J. T. Bernhard, "Beamsteering in pattern reconfigurable arrays using directional modulation," *IEEE Trans. Antennas Propag.*, vol. 58, no. 7, pp. 2259–2265, Jul. 2010.
- [7] J. Hu, F. Shu and J. Li, "Robust synthesis method for secure directional modulation with imperfect direction angle," *IEEE Commun. Lett.*, vol. 20, no. 6, pp. 1084–1087, Jun. 2016.
- [8] Y. Ding, Y. Zhang, and V. Fusco, "Fourier Rotman lens enabled directional modulation transmitter," *Int. J. Antennas Propag.*, vol. 2015, Article ID 285986, 13 pages, 2015.
- [9] N. Valliappan, A. Lozano, and R. W. Heath, "Antenna subset modulation for secure millimeter-wave wireless communication," *IEEE Trans. Commun.*, vol. 61, pp. 3231–3245, Aug. 2013.
- [10] N. N. Alotaibi and K. A. Hamdi, "Switched phased-array transmission architecture for secure millimeter-wave wireless communication," *IEEE Trans. Commun.*, vol. 64, no. 3, pp. 1303–1312, Mar. 2016.
- [11] Y. Ding, V. Fusco, and A. Chepala, "Circular directional modulation transmitter array," *IET Microw., Antennas Propag.*, vol. 11, no. 3, pp. 1909–1917, Oct. 2017.
- [12] Y. Ding and V. Fusco, "Development in directional modulation technology," *Forum for Electromagn. Res. Methods and Appl. Technol. (FERMAT)*, vol. 13, Jan.-Feb. 2016.
- [13] Y. Ding, J. Zhang, and V. Fusco, "Frequency diverse array OFDM transmitter for secure wireless communication," *Electron. Lett.*, vol. 51, no. 17, pp. 1374–1376, Aug. 2015.
- [14] W. H. Kummer, A. T. Villeneuve, T. S. Fong, and F. G. Terrio, "Ultra low sidelobes from time-modulated arrays," *IEEE Trans. Antennas Propag.*, vol. 11, no. 6, pp. 633–639, Nov. 1963.
- [15] B. Lewis and J. B. Evins, "A new technique for reducing radar response to signals entering antenna sidelobes," *IEEE Trans. Antennas Propag.*, vol. 31, no. 6, pp. 993–996, Jun. 1983.
- [16] W.-Q. Wang, H. So, and A. Farina, "An overview on time/frequency modulated array processing," *IEEE J. Sel. Topics Signal Process.*, vol. 11, no. 2, pp. 228–246, Mar. 2017.
- [17] C. He, X. Liang, Z. Li, J. Geng, and R. Jin, "Direction finding by time-modulated array with harmonic characteristic analysis," *IEEE Antennas Wireless Propag. Lett.*, vol. 14, no. 1, pp. 642–645, 2015.
- [18] C. He, X. L. Liang, B. Zhou, J. P. Geng, and R. H. Jin, "Space-division multiple access based on time-modulated array," *IEEE Antennas Wireless Propag. Lett.*, vol. 14, no. 1, pp. 610–613, 2015.
- [19] F. Shu, X. Wu, J. Hu, J. Li, R. Chen, and J. Wang, "Secure and precise wireless transmission for random-subcarrier-selection-based directional modulation transmit antenna array," *IEEE J. Sel. Areas Commun.*, vol. 36, no. 4, pp. 890–904, Apr. 2018.
- [20] Z. Chen, G. Gokeda, and Y. Yu: *Introduction to Direction-of-Arrival Estimation*, Norwood, MA, Artech House, 2010, 193 pages, ISBN 978-1-59693-089-6.
- [21] Y. Ding and V. Fusco, "Establishing metrics for assessing the performance of directional modulation systems," *IEEE Trans. Antennas Propag.*, vol. 62, no. 5, pp. 2745–2755, Feb. 2014.